0D Modeling of Liquid Atomization in a Two-Phase Flow

Sébastien Beneteau

Polytechnique Montréal
Fabian Denner, Bruno Savard

Abstract

This work aims to develop a robust model for the atomization modeling of a liquid jet. The adopted approach is deliberately 0D in physical space but multidimensional in phase space, in order to account for the temporal evolution of droplet size and velocity distributions. A numerical implementation was developed around the RD (Reitz & Diwakar) model, selected for its simplicity and consistency in most regimes. Two resolution approaches were tested: Monte-Carlo and CQMOM. The CQMOM approach, combined with a log-normal law for offspring and a breakup frequency derived from characteristic breakup times (*bag*, *shear*), allows rapid resolution while ensuring result consistency.

1. The Model

1.1 Choice of a 0D approach and phase space

The modeling approach adopted in this work originates from a fundamental choice: rather than resolving the full spatial dynamics of droplets in a 3D flow, we focus on the temporal evolution of their intrinsic state variables. Specifically, we consider the size and velocity of droplets as the primary indicators of their dynamical behavior under atomization processes.

We therefore define a **zero-dimensional (0D)** spatial framework, where no spatial resolution is considered, and instead operate within a **two-dimensional (2D) phase space** formed by the droplet radius r and velocity u. This choice implies the assumption of spherical droplets.

The initial step involves the temporal modeling of a *single droplet* in this (r, u) phase space. The aim is to understand how its size and velocity evolve over time due to aerodynamic and interfacial forces. At this scale, two main fragmentation mechanisms are typically considered: **primary atomization**, which involves the disintegration of a liquid sheet or jet into droplets, and **secondary atomization**, which concerns the breakup of already-formed droplets. In the context of this study where droplets are already formed and immersed in a gas stream, secondary atomization is the dominant mechanism, although primary breakup can still occur for large droplets, in the considered regimes.

Once the behavior of a single droplet is understood, the framework is extended to a *population of droplets*. So, we employ the **method of moments**, which allows us to track a finite set of integral quantities (moments) that characterize the distribution without resolving it explicitly.

1.2 General model description

The model seeks to solve a transport equation of a density function $f(r, u, t)$ subjected to drag (braking) and fragmentation (breakup) phenomena. In this study, *coalescence* and *evaporation* are ignored for simplicity. Before deriving the transport equations, we should keep in mind these transports equations set the dynamic evolution for one droplet.

1.2.1 Droplet transport equations

The temporal evolution of a droplet (r, u) is governed by a system of coupled differential equations. For each droplet, the evolution of radius r and velocity u follows:

$$\frac{dr}{dt} = \left(\frac{dr}{dt}\right)_{fragmentation} \tag{1}$$

$$\frac{du}{dt} = \left(\frac{du}{dt}\right)_{drag} \tag{2}$$

The drag term is modeled by the classical particle dynamics equation:

$$\left(\frac{du}{dt}\right)_{drag} = \frac{3}{8} C_D \frac{\rho_g}{\rho_l} \frac{1}{r} |u_g - u|(u_g - u) \tag{3}$$

where ρ_g and ρ_l are respectively the gas and liquid densities, and u_g is the ambient gas velocity. The drag coefficient C_D used is based on the classical empirical correlation proposed by Schiller and Naumann. It expresses C_D as a function of the Reynolds number Re. The drag coefficient is computed as:

$$C_D = \begin{cases} 2400\,(1 + 0.1315 \cdot 0.01^{a_1}) & \text{if } Re \leq 0.01, \\ \frac{24}{Re}\,(1 + 0.1315 \cdot Re^{a_2}) & \text{if } 0.01 < Re \leq 20, \\ \frac{24}{Re}\,(1 + 0.1935 \cdot Re^{0.6305}) & \text{if } 20 < Re \leq 260, \\ 0.444 & \text{if } Re > 260. \end{cases} \tag{4}$$

where $a_1 = 0.82 - 0.05\log_{10}(0.01)$ and $a_2 = 0.82 - 0.05\log_{10}(Re)$.

Throughout the simulations conducted in this work, the Reynolds number typically varied within the range:

$$0.1 \lesssim Re \lesssim 260,$$

which remains within the domain of validity of the Schiller–Naumann model, ensuring consistency with established low-to-intermediate Reynolds regimes encountered in droplet dynamics.

The fragmentation term $\left(\frac{dr}{dt}\right)_{fragmentation}$ is more complex and is the subject of the following subsection.

1.2.2 Reitz-Diwakar (RD) fragmentation model

The RD model relies on the evaluation of characteristic times to trigger droplet breakup. Two fragmentation modes are considered: the *bag* mode and the *shear* mode, each associated with a specific characteristic time.

The characteristic times are defined as follows:

$$\tau_{bag} = \pi\sqrt{\frac{\rho_l r^3}{2\sigma_l}} \tag{5}$$

$$\tau_{shear} = 1.8 \cdot r\sqrt{\frac{\rho_l}{\rho_g}} \cdot \frac{1}{|u_r|} \tag{6}$$

where σ_l is the liquid surface tension and $u_r = u - u_g$ is the relative velocity between the droplet and the gas.

For the determination of r_{child}, we introduce a new logic that consists in a stochastic approach for the number of child droplets formed and their radius. This approach is more detailed in the next part. Then, we have :

$$r_{child} = 0.681 \cdot r \ , \ 0.681 = \frac{1}{(2.17+1)^{1/3}} \tag{7}$$

where 2.17 is the mean value of the discrete log-normal distribution of the number of child droplets formed.

Now, we can derive the final model for the droplet radius evolution :

$$\frac{dr}{dt} = H(We_g - We_{crit})(r_{child} - r)\times \left(\frac{H(We_g - 6)(1 - H(\xi - 0.5))}{\tau_{bag}} + \frac{H(\xi - 0.5)}{\tau_{shear}}\right) \tag{8}$$

where $\xi = We_g/\sqrt{Re_g}$, $We_{crit} = 12(1 + 1.077Oh^{1.6})$ is the fragmentation criterion, and H is the Heaviside function. The We_{crit} formula and criteria comes from the Pilch and Erdman theory on atomization of droplets and we choose to keep it in order to have a threshold in our evolution.

To conclude with this section, we now have the dynamic equations for the evolution of one droplet for each phase variable. Therefore, we can be interested in solving these equations for a population of droplets with, as we said before, the method of moments. We will be focusing on the CQMOM approach and the Monte-Carlo approach.

2. CQMOM method with fragmentation source term

The CQMOM (Conditional Quadrature Method of Moments) method allows solving the transport equation of the probability density function $f(r, u; t)$ by solving the dynamic equations of each moments of our droplet distribution.

2.1 Moment evolution

The dynamic equation of moments M_{ij} is written as:

$$\frac{\partial M_{ij}}{\partial t} = \underbrace{\sum_k w_k f_k^{(i,j)}}_{\text{Transport}} + \underbrace{S_{ij}}_{\text{Fragmentation source}} \tag{9}$$

where $\{w_k, r_k, u_k\}$ are the CQMOM quadrature weights and nodes, and S_{ij} is the fragmentation source term. With the method of moments approach, it is current to gather all the breakup or fragmentation processes in the source term and not in the transport term anymore. By doing so, the transport term only contained the drag phenomena and :

$$\frac{dr}{dt} = 0 \tag{10}$$

However, our evolution with the RD model is still going to be useful in the source term and in the Monte-Carlo approach. Effectively, the variation of the radius will be guaranteed by the source term and so, we no longer need this variation in the transport term. Basically, if we have forgotten to remove the variation of radius in the transport term, we will simply notice in the simulation its effect to be two times bigger.

2.2 Source term formulation

The source term S_{ij} represents the contribution of fragmentation to moment evolution. In the litterature and in opposite to our Monte-Carlo model, parent droplets die during breakup. Therefore, the number of child droplets is greater than 2 and we choose it here to be in range [2, 6]. It will follow a discrete log-normal distribution with parameters $\mu = 3$ and $\sigma = 1$. The source term can be expressed as:

$$S_{ij} = \sum_k w_k \left[\underbrace{B_{ij}(r_k, u_k; t)}_{\text{Birth}} - \underbrace{D_{ij}(r_k, u_k; t)}_{\text{Death}}\right] \tag{11}$$

The birth term $B_{ij}(r_k, u_k; t)$ models the appearance of new droplets from fragmentation. It is written as:

$$B_{ij}(r_k, u_k; t) = N_{frag} \cdot \Gamma(r_k, u_k; t) \cdot I_{ij}(r_k, u_k) \tag{12}$$

The $I_{ij}(r_k, u_k)$ term refered to the result of the i^{th} moment of the child size distribution times u_k^j. Basically, the child size distribution can be refer as the probability of a droplet (r'_k, u'_k) to form a child droplet (r_k, u_k). But, we assume the child droplets to have the same speed as their parents. So, the child size distribution only depends on the radius and will follow a log-normal distribution. This term is expressed as:

$$I_{ij}(r_k, u_k) = u_k^j \left(\frac{3}{4\pi}\right)^{i/3} \exp\left(\frac{i\mu_k}{3} + \frac{1}{2}\left(\frac{i\sigma_k}{3}\right)^2\right) \tag{13}$$

with the parameters coming from the daughter droplet sizes distribution:

$$\mu_k = \ln\left(\frac{V_{mean,k}^2}{\sqrt{\sigma_{V_k}^2 + V_{mean,k}^2}}\right) \ , \ \sigma_k \ = \sqrt{\ln\left(1 + \frac{\sigma_{V_k}^2}{V_{mean,k}^2}\right)} \tag{14}$$

where $V_{mean,k} = \frac{V_k}{N_{frag}}$, $\sigma_{V_k} = \frac{V_k}{(N_{frag})\times 12}$, $V_k = \frac{4}{3}\pi r_k^3$.

Next, $N_{frag} \approx 3.4$ is the average number of daughter droplets for our log-normal distribution in range [2,6], and $\Gamma(r_k, u_k)$ is the fragmentation rate, written as:

$$\Gamma(r_k, u_k; t) = H(We_g - We_{crit})\times \left(\frac{H(We_g - 6)(1 - H(\xi - 0.5))}{\tau_{bag}} + \frac{H(\xi - 0.5)}{\tau_{shear}}\right) \tag{15}$$

In the fragmentation rate term, we can recognize the influence of the RD model with the use of the characteristic times introduced earlier.

The death term $D_{ij}(r_k, u_k; t)$ represents the disappearance of the mother droplet. It is written as:

$$D_{ij}(r_k, u_k; t) = r_k^i \cdot u_k^j \cdot \Gamma(r_k, u_k; t) \tag{16}$$

3. Monte Carlo approach

To validate the CQMOM model, a Monte Carlo approach was implemented. This method explicitly simulates each droplet and its fragmentation processes. The dynamic of each droplet is described exactly as in our RD model, with the variation of speed and radius. The Monte Carlo algorithm follows the following steps:

1. **Fragmentation detection:** For each droplet, those criterias are verified:
   - Frequency criteria : fragmentation occurs at a frequency $\frac{1}{\tau_{bag}}$ ou $\frac{1}{\tau_{sheer}}$ for each droplet as the RD model implies.
   - Volume criteria : $\sum V_{current} \leq V_{initial}$ in order to prevent an excessive creation of droplets that will not respect mass conservation of the system.
   - Number criteria : $N_{droplets} \leq 200$ for one initial droplet for memory issues in the simulation. By the way, this threshold is almost never attained.
   - Weber criteria : $We > We_{crit}$ inherited from the Pilch and Erdman theory and our RD model.
2. **Determination of daughter droplet number:** A truncated discrete log-normal distribution is used with $\mu = 2$ and $\sigma = 1$, favoring fragmentation into 2 or 3 droplets in the domain which correspond in this case of the values 1 and 2 in the range $[1, 5]$ as the parent droplet remains alive, in contrast with the CQMOM approach.
3. **Calculation of daughter droplet sizes:** A log-normal volume distribution is applied for a droplet k:

$$\mu_{V_k} = \frac{V_{initial,k}}{N_{daughters,k} + 1} \tag{17}$$

$$\sigma_{V_k} = \frac{\mu_{V_k}}{12} \tag{18}$$

   Strict mass conservation is imposed with the constraint $\sum V_{daughter} < 0.95 \cdot V_{initial}$. Here, the parent droplet must remain alive so we need to impose an upper limit to the volume of the daughters droplets, in order to keep a consistent size for the parent.
4. **Iterative process:** The process is repeated for each daughter droplet until the fragmentation criterion is no longer satisfied.

To conclude with this section, notice that, as the Monte-Carlo approach simulates each droplet, we will observe discrete fragmentation events whereas in the CQMOM approach, the fragmentation effect are continuous. The more the number of initial droplet is high, the more those discrete events will tend to a continuous-type process and so, towards the CQMOM solution.

4. Configuration and simulation parameters

4.1 Injection conditions

The injection conditions set the initial dynamic state of the droplets. These include the initial radius of the droplets, their injection velocity, and the ambient gas velocity. Depending on the chosen regime—low-pressure or high-pressure injection—these parameters significantly influence the subsequent evolution of the spray. A high injection velocity will favor more intense secondary atomization and shift the droplet size distribution toward smaller radii,

whereas a low injection velocity may delay or even suppress breakup mechanisms. The initial droplet radius also defines the initial Weber and Reynolds numbers, hence directly impacting the fragmentation potential. In practice, these conditions must be carefully tuned to match the target physical scenario and available computational resources.

4.2 Thermodynamic conditions

The gas thermodynamic conditions—namely, pressure and temperature—are essential as they affect both fluid properties and interaction regimes. Higher ambient temperatures reduce the viscosity of the gas and can accelerate breakup through enhanced aerodynamic forces. Similarly, pressure influences gas density, thus modifying both the Reynolds and Weber numbers. These conditions must be defined consistently with the injection system and surrounding environment, particularly when modeling fuel injection in engines or combustors.

4.3 Fluid physical properties

The liquid and gas properties play a crucial role in the evolution of droplets. The density and viscosity of the gas determine the aerodynamic drag and fragmentation mechanisms, while the liquid's density, viscosity, and surface tension govern the internal resistance to breakup. These parameters enable modeling different injection media—from water to various fuels or complex fluids. It is also possible to simulate different gases (e.g., air, nitrogen, or combustion gases) by adjusting the gas properties accordingly. The liquid surface tension is set to σ_l N/m in the simulation.

4.4 Characteristic dimensionless numbers

To ensure the physical relevance and consistency of the simulation, several dimensionless numbers are monitored. The **Weber number** (We) is central, as it quantifies the ratio between aerodynamic forces and surface tension forces; it serves as the principal indicator for the onset of droplet breakup. A critical Weber number, We_{crit}, defines the threshold above which atomization is likely to occur. The **Reynolds number** (Re) characterizes the relative importance of inertial to viscous forces and influences the drag coefficient and the fragmentation criteria with its appearance in the Ohnesorge number. The **Ohnesorge number** (Oh) captures the relative effect of viscosity compared to inertia and surface tension, and is particularly important to model the viscous effects in the fragmentation processes. Monitoring these numbers allows us to categorize the operating regime, to assess whether droplet fragmentation is physically justified and basically build our atomization model.

4.5 Numerical simulation parameters

The numerical setup of the simulation must balance accuracy and computational efficiency. The time step must be small enough to resolve the fast dynamics of droplet deformation and breakup. In this work, time steps are chosen in the range of 1 microseconds, more or less, with an upper bound around 20 microseconds for the coarsest configurations. The total simulated time typically ranges from 1 to 10 milliseconds, sufficient to capture atomization events. The number of output frames is determined by the total duration divided by the time step.

The number of initial droplets defines the scale of the simulation. For preliminary tests, it is advisable to start with 5 to 10 droplets, which already offer insightful dynamics with minimal computational cost. For more comprehensive studies, this number can be increased to over 100 droplets, or even 1000 if computational resources allow. However, increasing droplet count significantly increases memory usage and simulation time for the Monte-Carlo approach specifically. For this reason, a maximum number of droplets is set a priori here, approximately 200 newly created fragmentation droplets for one initial drop, to cap memory allocation as we said before.

The simulation uses the **DOP853** integration scheme, an explicit 8th-order Runge-Kutta method with adaptive time stepping.

4.6 Initial distribution

The initial droplet population is defined statistically in phase space. Each droplet is initialized with a mean radius and velocity vector, denoted $\mu = [r_0, u_0]$, corresponding respectively to the typical droplet size and injection velocity. To introduce physical variability and model polydispersity, a Gaussian distribution is applied around this mean. The standard deviation (or variance) controls the level of dispersion: for near-monodisperse sprays, variance levels around 5 to 10% at most are used, while more polydisperse sprays starts at 10% and may reach 20 to 25%. Moreover, the variance of the radius and the one of the velocity is, often, not the same. Usually, we observe much dispersion for radius than for velocities. In my work, I chose a 10% dispersion on radius and a 5% dispersion on velocity. Finally, this initial distribution plays a key role in determining the initial spread of phase space trajectories and ultimately affects the overall atomization behavior.

5. Results

This section presents the numerical results we can obtain with our 0D modeling of liquid atomization. These results are just examples to visualize what type of results we can expect from this work.

5.1 Visualize the evolution of moments and characteristic quantities

The moment-based approach uses moments to represent the droplet population. But, we need to give to each of

these moments a physical meaning in order to understand and analyze the results. They are defined as:

Moment	Definition	Physical Meaning
M_{00}	$\sum w_k$	Total number of droplets
M_{10}	$\sum w_k \times r_k$	Weighted sum of radii
M_{01}	$\sum w_k \times u_k$	Weighted sum of velocities
M_{11}	$\sum w_k \times r_k \times u_k$	Mixed moment (covariance)

Table 1: Moments and their physical meaning

Where w_k, r_k, and u_k are respectively the weight, radius, and velocity of droplet k. Now, we can defined new quantities that we will be more useful for us. These quantities are the mean radius and the mean velocity of the distribution and are calculated as follows:

$$\text{mean radius} = \frac{M_{10}}{M_{00}} \text{ , mean velocity} = \frac{M_{01}}{M_{00}} \tag{19}$$

The mixed moment M_{11} provides insight into radius-velocity correlation in the population.

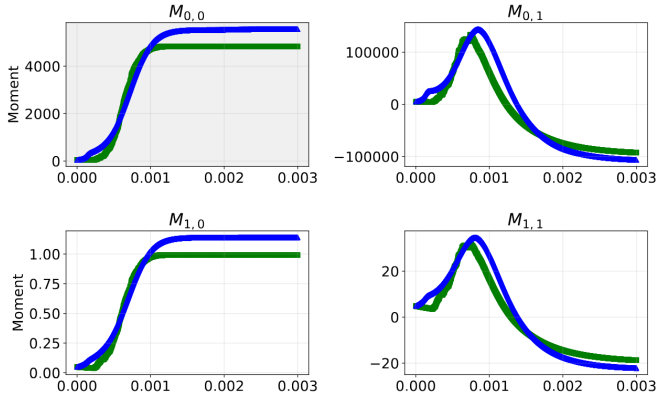

Figure 1: Evolution of mixed moments M_{ij} over 3 milliseconds: MC (green) vs CQMOM (blue)

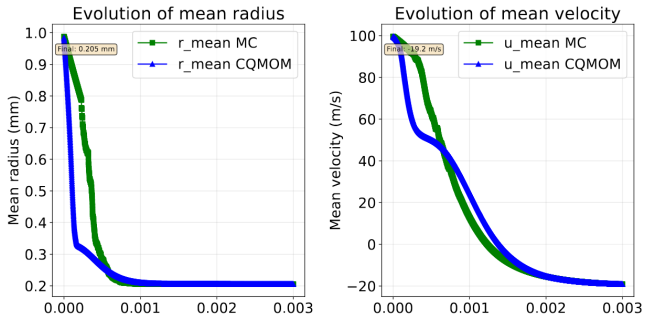

Figure 2: Evolution of mean radius (left) and mean velocity (right) over 3 milliseconds: MC (green) vs CQMOM (blue)

Figure 1 illustrates the temporal evolution of the four lowest-order moments $M_{0,0}$, $M_{0,1}$, $M_{1,0}$, and $M_{1,1}$ over a 3 ms simulation time. The initial exponential growth of $M_{0,0}$, which corresponds to the total number of droplets, is directly associated with the fragmentation process. As droplets undergo breakage, their number increases rapidly until the Weber number falls below the critical value We_{crit} defined by the Pilch and Erdman criterion. This threshold effectively stabilizes the droplet population, as further breakage is inhibited.

The behavior of $M_{1,0}$, the weighted sum of droplet radii, mirrors that of $M_{0,0}$, though its magnitude remains small. This is expected, as the breakage process generates smaller daughter droplets while conserving mass, leading to many droplets with reduced radius contributing to the moment. Importantly, $M_{1,0}$ does not directly reflect a decrease in average radius, but rather the cumulative sum of radii weighted by the particle weights.

The evolution of $M_{0,1}$, the weighted sum of droplet velocities, exhibits a sharp increase during the early fragmentation phase. Since daughter droplets initially inherit the same velocity as their parent, the creation of more particles leads to a net increase in $M_{0,1}$. However, as the simulation progresses, drag forces begin to dominate and cause a progressive deceleration of droplets. This effect results in a gradual decline of $M_{0,1}$, which eventually stabilizes as the velocities converge toward a terminal regime.

Regarding the mixed moment $M_{1,1}$, which combines the effects of both droplet radius and velocity, its evolution is dominated by the contribution of $M_{0,1}$. Due to the relatively small magnitude of $M_{1,0}$ compared to $M_{0,1}$, the trend of $M_{1,1}$ closely follows that of the velocity moment.

Figure 2 shows the evolution of the mean radius and mean velocity, two physically interpretable quantities derived from the moment definitions. The mean radius decreases sharply in the early phase of the simulation, exhibiting a nearly linear trend that aligns with predictions from the RD model. This decrease continues until the system reaches the critical Weber threshold, at which point fragmentation slows and the rate of radius reduction decreases. Thereafter, the evolution is governed primarily by drag-induced changes in the velocity field, which indirectly influence the Weber number and thus the continuation of breakage events. The stabilization of the mean radius coincides with the plateau observed in the $M_{0,0}$ curve, indicating the end of the fragmentation process.

The mean velocity also follows a rapid decline initially. Notably, in the CQMOM simulation, a temporary plateau appears after the initial drop. This is interpreted as the point at which the breakage process halts (due to the critical Weber number being reached), causing a transition from fragmentation-driven dynamics to drag-dominated deceleration. The drag continues to act on the population, slowly reducing the velocity until stabilization is achieved.

Overall, the close agreement between the Monte-Carlo (MC) and CQMOM results across all presented metrics provides strong validation of the moment-based method and confirms its ability to accurately capture the dynamics of the droplet population.

5.2 Temporal evolution of size distributions

The temporal evolution of the droplet radius distribution reveals a characteristic three-phase process, driven by the underlying fragmentation dynamics.

Initially, the distribution is dominated by a single mode corresponding to the injected droplet population. As fragmentation starts, a second mode begins to emerge at smaller radii, corresponding to the newly generated child droplets. During this stage, the initial mode remains dominant, while the nascent secondary mode has a much lower amplitude. The propagation of the droplet population toward smaller radii is gradual, forming a "wave" in the histogram.

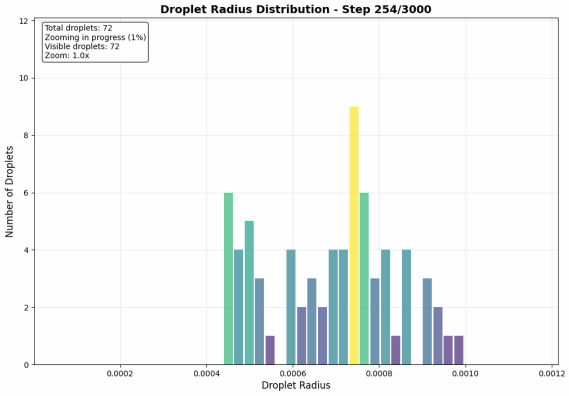

Figure 3: Initialization and onset of fragmentation

As time progresses, the number of droplets in the smaller-radius mode increases, while the population in the larger-radius mode decreases due to continued fragmentation. Eventually, a crossover occurs: the initially small-amplitude mode at smaller radii becomes the dominant peak, while the former main mode at larger radii becomes secondary. This inversion of dominance marks the transition to the intermediate stage of the process.

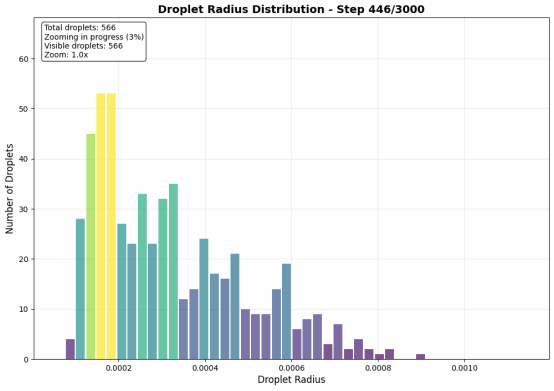

Figure 4: Mode inversion of the distribution

In the final stage, the distribution reaches a quasi-steady shape. The dominant mode is now the one at small radii, and the secondary mode at larger radii has disappeared. The resulting distribution exhibits a log-normal shape, consistent with the stochastic nature of the chosen break-up process.

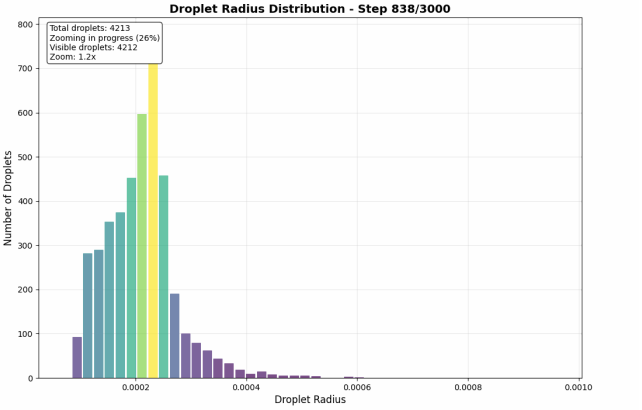

Figure 5: Final stage and stabilization of the evolution

However, by zooming on the distribution, we can actually distinguish kind of two modes in this distribution, that are centered at slightly different radius. That's why this log-normal looking distribution looks a bit flat on the smaller radius part.

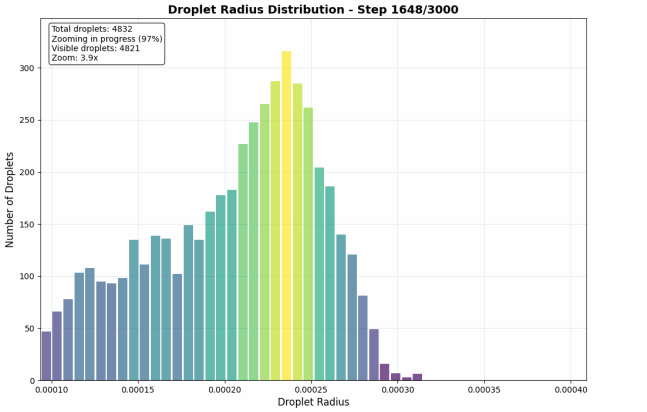

Figure 6: Final distribution

From a practical standpoint, the observation of the bimodal structure depends on the number of droplets in the population. Below roughly ten droplets, the secondary mode is difficult to distinguish due to statistical limitations. Between about ten and one hundred droplets, the bimodal pattern becomes clearly visible, with the crossover phase being particularly evident when the population size is closer to one hundred droplets.

6. Conclusion

In this work, a complete zero-dimensional (0D) framework for modeling the secondary atomization of liquid droplets has been developed and assessed. The model is built upon

the Reitz–Diwakar (RD) formulation, enhanced by the use of a stochastic log-normal offspring distribution and a critical Weber number criterion from the Pilch–Erdman theory. Two distinct numerical strategies were implemented and compared:

- A **Monte Carlo** approach, explicitly resolving individual droplets and their stochastic fragmentation events.
- A **CQMOM** (Conditional Quadrature Method of Moments) approach, in which breakup effects are incorporated into a dedicated source term, enabling efficient tracking of distribution moments without resolving the full population.

The systematic cross-comparison of both methods demonstrated excellent agreement in the evolution of global quantities (moments, mean radius, mean velocity) and in the temporal development of droplet size distributions. This validates the CQMOM formulation as a reliable and computationally attractive.

Beyond the numerical agreement, the model successfully reproduces the characteristic three-phase evolution of droplet radius distributions—from the emergence of a secondary mode, through mode inversion, to the final stabilized state—consistent with the physics of secondary breakup.

Overall, the present work establishes a solid basis for efficient and accurate simulation of droplet population dynamics in atomization problems. Future developments may focus on extending the framework to include additional physical processes such as coalescence, evaporation, or coupling with spatially resolved gas-phase fields, thereby broadening its range of applicability.

A. Mathematical Derivation of CQMOM formulation

The transport equation for the probability density function $f(r,u;t)$ is given by:

$$\frac{\partial f(r,u;t)}{\partial t}+\frac{\partial}{\partial u}\left(\dot{u}(r,u;t)f(r,u;t)\right)=B^{br}(r,u;t)-D^{br}(r,u;t) \tag{20}$$

The moments of the distribution are defined as:

$$M_{ij}(t)=\int_{\Omega_r}\int_{\Omega_u} r^i u^j f(r,u;t)\,dr\,du \tag{21}$$

where $\Omega_r=[0,\infty[$ and $\Omega_u=[u_g,\infty[$, $(i,j)\in\mathbb{N}^2$.
The temporal evolution of moments is given by:

$$\begin{aligned}\frac{dM_{ij}(t)}{dt} =& -\int_{\Omega_r}\int_{\Omega_u} r^i u^j \frac{\partial}{\partial u}\left(\dot{u}(r,u;t)f(r,u;t)\right)\,dr\,du \\ &+\int_{\Omega_r}\int_{\Omega_u} r^i u^j \left(B^{br}(r,u;t)-D^{br}(r,u;t)\right)dr\,du\end{aligned} \tag{22}$$

We are further interested in the derivation of the source term for the breakup process. The birth term due to fragmentation is expressed as:

$$\begin{aligned}B^{br}(r,u;t)=&\int_{\Omega_r}\int_{\Omega_u} N_{\text{daughter}}(r',u';t)\,P(r,u\mid r',u';t) \\ &\times\Gamma(r',u';t)\,f(r',u';t)\,dr'\,du'\end{aligned} \tag{23}$$

where:

- $N_{\text{daughter}}(r',u';t)$: number of daughter droplets generated by a droplet of state (r',u')
- $P(r,u\mid r',u';t)$: probability density that a daughter droplet (r,u) originates from a parent droplet (r',u')
- $\Gamma(r',u';t)$: fragmentation frequency of a droplet (r',u')

The death term represents the disappearance of parent droplets:

$$D^{br}(r,u,t)=\Gamma(r,u;t)\cdot f(r,u;t) \tag{24}$$

We should now precise all the terms in the birth term. The following assumptions are made:

- $N_{\text{daughter}}(r',u';t)=N_{\text{daughter}}\in[2,6]$ (mean value of a discrete log-normal distribution)
- For $P(r,u\mid r',u';t)$, we will assume that it only depends on the size of the droplets, independently of time and speed. So, the velocity of the child droplets will be the same as their parents. Moreover, in order to respect the conservation of mass, the distribution will be based on the volume x of the droplet and a variable change will be needed in the calculation. Therefore :

$$P(x\mid x')=\frac{1}{x\sigma\sqrt{2\pi}}\exp\left(-\frac{(\ln(x)-\mu)^2}{2\sigma^2}\right) \tag{25}$$

with parameters:

$$\begin{aligned}\mu&=\ln\left(\frac{x'_{mean}}{\sqrt{\sigma_x^2+(x'_{mean})^2}}\right)\\ \sigma&=\sqrt{\ln\left(1+\frac{\sigma_x^2}{(x'_{mean})^2}\right)}\\ x_{mean}&=\frac{x'}{N_{daughter}},\quad \sigma_x=\frac{x_{mean}}{12}\end{aligned} \tag{26}$$

- With respect of our RD fragmentation model, the breakage rate can be described as:

$$\begin{aligned}\Gamma(r,u;t)=&H(We_g-We_{crit})\\ &\times\left[H(We_g-6)(1-H(\xi-0.5))\frac{1}{\tau_{bag}}\right.\\ &\left.+H(\xi-0.5)\frac{1}{\tau_{shear}}\right]\end{aligned} \tag{27}$$

where H is the Heaviside function

Before gathering these elements, we must now derive the hypothesis made by the CQMOM approximation which is the following

$$f(r,u;t) = \sum_k w_k\, \delta(r - r_k(t))\, \delta(u - u_k(t)) \tag{28}$$

where w_k are called the weights, $r_k(t), u_k(t)$ are the nodes of our quadrature and δ the Dirac distribution.

Then, the birth source term becomes:

$$\begin{aligned}
&\iint_{\Omega_r\Omega_u} r^i u^j\, B^{br}(r,u;t)\, dr\, du \\
&= \sum_k w_k N_{\text{daughter}} \int_{\Omega_r}\int_{\Omega_u}\int_{\Omega_r}\int_{\Omega_u} r^i u^j\, \delta(u-u')\, P(r \mid r') \\
&\quad \times \Gamma(r',u';t)\, \delta(r' - r_k(t))\, \delta(u' - u_k(t)) \\
&\quad \times dr\, du\, dr'\, du'
\end{aligned} \tag{29}$$

By noticing the Dirac distribution is the neutral element of the convolution, and by assuming that our functions can be extended on $\mathbb{R}$, which is true in our case, we obtain:

$$\begin{aligned}
&\iint_{\Omega_r\Omega_u} r^i u^j\, B^{br}(r,u;t)\, dr\, du \\
&= \sum_k w_k N_{\text{daughter}}\, \Gamma(r_k,u_k;t) \int_{\Omega_r}\int_{\Omega_u} r^i u^j\, \delta(u-u_k) \\
&\quad \times P(r \mid r_k)\, dr\, du
\end{aligned} \tag{30}$$

Therefore, we isolate the calculation of the integrals by respect of r and u. For the velocity, we can use the same argument that earlier with the Dirac. For the radius, we recognize the i^{th} moment of a probability density function and here, of a log-normal distribution. Without forgetting the variable change, we now have:

$$\begin{aligned}
&\iint_{\Omega_r\Omega_u} r^i u^j\, B^{br}(r,u;t)\, dr\, du \\
&= \sum_k w_k N_{\text{daughter}}\, \Gamma(r_k,u_k;t)\, u_k^j \\
&\quad \times \left(\frac{3}{4\pi}\right)^{\frac{i}{3}} \exp\left(\frac{i\mu_k}{3} + \frac{1}{2}\left(\frac{i\sigma_k}{3}\right)^2\right)
\end{aligned} \tag{31}$$

with parameters:

$$\begin{aligned}
\mu_k &= \ln\left(\frac{x'_{mean,k}}{\sqrt{\sigma_{x,k}^2 + (x'_{mean,k})^2}}\right) \\
\sigma_k &= \sqrt{\ln\left(1 + \frac{\sigma_{x,k}^2}{(x'_{mean,k})^2}\right)} \\
x_{mean,k} &= \frac{x_k}{N_{daughter}}, \quad \sigma_{x,k} = \frac{x_{mean,k}}{12}
\end{aligned} \tag{32}$$

Now, we derive the death source term, more easily:

$$\begin{aligned}
&\iint_{\Omega_r\Omega_u} r^i u^j\, D^{br}(r,u;t)\, dr\, du \\
&= \sum_k w_k r_k^i u_k^j\, \Gamma(r_k,u_k;t)
\end{aligned} \tag{33}$$

These expression form the basis for the CQMOM implementation of the fragmentation source term used in the numerical simulations.